

UNCLASSIFIED

AD NUMBER

AD315671

CLASSIFICATION CHANGES

TO: UNCLASSIFIED

FROM: CONFIDENTIAL

LIMITATION CHANGES

TO:
Approved for public release; distribution is unlimited.

FROM:
Distribution authorized to U.S. Gov't. agencies and their contractors;
Administrative/Operational Use; MAR 1960. Other requests shall be referred to Arnold Engineering Development Center, Arnold AFB, TN.

AUTHORITY

ASTIA Tab No. Bulletin 70-21, dtd 1 Nov 1970;
ASTIA Tab No. Bulletin 70-21, dtd 1 Nov 1970

UNCLASSIFIED

AD NUMBER

AD315671

CLASSIFICATION CHANGES

TO:

CONFIDENTIAL

FROM:

SECRET

AUTHORITY

31 Mar 1963, Group-3, DoDD 5200.10

THIS PAGE IS UNCLASSIFIED

UNCLASSIFIED

AD. 315671

DEFENSE DOCUMENTATION CENTER

FOR

SCIENTIFIC AND TECHNICAL INFORMATION

CAMERON STATION ALEXANDRIA, VIRGINIA

CLASSIFICATION CHANGED
TO UNCLASSIFIED
FROM CONFIDENTIAL
PER AUTHORITY LISTED IN

BULL. 70-21 1 NOV. 1970



UNCLASSIFIED

SECRET

AD

- L

3 1 5 6 7 1

Reproduced by

Armed Services Technical Information Agency

ARLINGTON HALL STATION; ARLINGTON 12 VIRGINIA

NOTICE: WHEN GOVERNMENT OR OTHER DRAWINGS, SPECIFICATIONS OR OTHER DATA ARE USED FOR ANY PURPOSE OTHER THAN IN CONNECTION WITH A DEFINITELY RELATED GOVERNMENT PROCUREMENT OPERATION, THE U. S. GOVERNMENT THEREBY INCURS NO RESPONSIBILITY, NOR ANY OBLIGATION WHATSOEVER; AND THE FACT THAT THE GOVERNMENT MAY HAVE FORMULATED, FURNISHED, OR IN ANY WAY SUPPLIED THE SAID DRAWINGS, SPECIFICATIONS, OR OTHER DATA IS NOT TO BE REGARDED BY IMPLICATION OR OTHERWISE AS IN ANY MANNER LICENSING THE HOLDER OR ANY OTHER PERSON OR CORPORATION, OR CONVEYING ANY RIGHTS OR PERMISSION TO MANUFACTURE, USE OR SELL ANY PATENTED INVENTION THAT MAY IN ANY WAY BE RELATED THERETO.

SECRET

AD No. 315671

ASTIA FILE COPY

FILE COPY

Return to

ASTIA

ARLINGTON HALL STATION
ARLINGTON 12, VIRGINIA

Attn: TISS

NOX

(TITLE UNCLASSIFIED)

FORCE TESTS OF LENTICULAR CONFIGURATIONS AT SUPERSONIC SPEEDS

By
A. Anderson
VKF, ARO, Inc.

March 1960

ARNOLD ENGINEERING DEVELOPMENT CENTER

AIR RESEARCH AND DEVELOPMENT COMMAND



ASTIA
RECEIVED
MAR 24 1960
TIPDR
A

SECRET

AEDC-TN-60-51

(Title Unclassified)
FORCE TESTS
OF LENTICULAR CONFIGURATIONS
AT SUPERSONIC SPEEDS

By

A. Anderson
VKF, ARO, Inc.

CLASSIFIED DOCUMENT

"This material contains information affecting the national defense of the United States within the meaning of the Espionage Laws, Title 18, U.S.C., Sections 793 and 794, the transmission or revelation of which in any manner to an unauthorized person is prohibited by law."

March 1960

ARO Project No. 331977

Contract No. AF 40(600)-800

SECRET

OTHERS

*... TO ...
A.E.D.C. - RECL*

CONTENTS

	<u>Page</u>
ABSTRACT	3
NOMENCLATURE	3
INTRODUCTION	5
APPARATUS	
Wind Tunnel	5
Models	5
Instrumentation	6
PROCEDURE	6
PRECISION OF DATA	7
RESULTS	8
CONCLUSIONS	9
REFERENCES	9

TABLE

1. Summary of Test Configurations	10
---	----

ILLUSTRATIONS

Figure

1. Tunnel A, a 40 by 40-in. Supersonic Wind Tunnel . . .	11
2. Sketches of Models	12
3. Sketches of Typical Model Installation and Model Components	13
4. Model Photographs	14
5. Longitudinal Characteristics of Basic Models at Mach 5.	16
6. Variation of Model Aerodynamic Parameters with Mach Number.	17
7. Longitudinal Stability and Control Characteristics at Mach 5.	18
8. Variation of Pitchvator Effectiveness with Mach Number	19
9. Lateral Stability and Control Characteristics at Mach 5, Model B3	20
10. Typical Schlieren Photographs	21

ABSTRACT

Longitudinal and lateral characteristics were obtained on four models of lenticular shape at Mach numbers 2, 3, 4, 5, and 6. The effectiveness of longitudinal and lateral control surfaces on the lenticular-shaped body is shown.

NOMENCLATURE

A_b	Base area, 2.84 sq in.
B	Body
C	Conevator
C_A	Axial-force coefficient, $C_{A_t} - C_{A_b}$
C_{A_b}	Base axial-force coefficient, $(p_\infty - p_b) A_b / qS$
C_{A_t}	Total axial-force coefficient, total axial force/ qS
C_D	Drag coefficient, drag/ qS
C_l	Rolling-moment coefficient, rolling moment/ qSc
C_L	Lift coefficient, lift/ qS
C_m	Pitching-moment coefficient, pitching moment/ qSc (see Fig. 2 for moment reference point)
C_N	Normal-force coefficient, normal force/ qS
C_n	Yawing-moment coefficient, yawing moment/ qSc (see Fig. 2 for moment reference point)
C_Y	Side-force coefficient, side force/ qS
c	Model diameter, 20.0 in. (except for Model B ₄ where c = 19.137 in.)
i_F/i_A	Deflection of forward and aft pitchvators, deg
M	Mach number
P	Pitchvator
p_b	Base pressure, psia
p_o	Free-stream stagnation pressure, psia

p_{∞}	Free-stream static pressure, psia
q	Free-stream dynamic pressure, psia
$Re/in.$	Unit Reynolds number
S	Model planform area, 314.16 sq in. (except Model B ₄ where $S = 288.0$ sq in.)
W	Wedgevator
α	Angle of attack, deg
δ_L/δ_R	Differential deflection angle of left and right wedgevators or conevators
ψ	Angle of yaw, deg
ϕ	Angle of roll, deg
ω_L/ω_R	Enclosed angle of left and right wedgevators or conevators

INTRODUCTION

Tests were conducted in Tunnel A of the von Karman Gas Dynamics Facility (VKF), Arnold Engineering Development Center, during the periods from September 8 to October 2 and from October 21 to October 30, 1959, for the Pomona Division of Convair at the request of the Air Proving Ground Center (APGC), Eglin Air Force Base.

The tests were made in support of a feasibility study by Convair of the Pye Wacket, a lenticular-shaped, air-to-air rocket. Initial investigations of the lenticular-shaped body by APGC were conducted in Tunnel E-1 of the VKF and are reported in Refs. 1, 2, and 3.

The primary test objective was to measure the drag and stability characteristics of four lenticular configurations at Mach numbers from 2 to 6 and to determine the effectiveness of various devices for pitch, yaw, and roll control of the lenticular-shaped body.

APPARATUS

WIND TUNNEL

Tunnel A (Fig. 1) is a 40 by 40 inch, continuous, closed circuit, variable-density, supersonic wind tunnel with a Mach number range from 1.5 to 6. The top and bottom walls of the nozzle are flexible plates which are automatically positioned at the desired contours by electrically driven screw-jacks. The tunnel is driven by a 100,000 horsepower compressor system which provides maximum tunnel stagnation pressures of 2 to 13.5 atmospheres at $M = 1.5$ and $M = 6$, respectively. Minimum operating pressures are less than one-tenth of the maximum. A complete description of the tunnel may be found in Ref. 4.

MODELS

The models, which were furnished by Convair, were fabricated of aluminum. Three basic body configurations (B_1 , B_2 , and B_3) with circular planforms 20 inches in diameter were fabricated (Fig. 2). Configuration B_4 was constructed from the B_1 body by blunting the leading edge.

Manuscript released by author February 1960.

Each body was provided with pitchvators for pitch control, located as shown in Fig. 2. Pitchvators of three different planforms and three different deflection angles were tested (see Fig. 3). Wedges and cones for lateral control were tested on Model B₃ (see Fig. 2). For yaw control the included angle of one wedge was of larger magnitude than the other to produce differential drag. Both the wedges and cones were differentially deflected for roll control (see Fig. 3, which includes a sketch of a typical model-balance installation). Installation photographs of models B₁ and B₃ are given in Fig. 4.

INSTRUMENTATION

An internal, six-component, 1.5-in.-diam., strain-gage balance fabricated by Task Corporation and furnished by Convair was calibrated at VKF. The gage signals from the balance were measured with 400-cps, null-balance, servo-potentiometers equipped with electrical digitizers which transmitted the signals to an ERA 1102 computer.

Absolute base pressure was measured with a differential pressure transducer which had essentially a vacuum for a reference pressure. The transducer output was measured with a d-c millivolt digitized recorder, which also served as the input to the computer.

Other data items, such as angle of attack and stagnation temperature and pressure, were measured, digitized, and automatically recorded.

PROCEDURE

Force and moment data at angles of attack from -5 to +15 deg were obtained for the configurations listed in Table 1. This table also lists the Mach numbers and roll angles at which data was measured for each configuration. The test conditions at each Mach number are listed in the table on the following page.

<u>M</u>	<u>p₀, psia</u>	<u>T₀, °R</u>	<u>Re/in. x 10⁶</u>
2	8	550	0.17
	12		0.25*
	15		0.31
3	20	560	0.25
	29		0.36*
	32		0.39
4	27	585	0.19
	47		0.31
	68		0.45*
5	60	640	0.23
	105		0.36
	150		0.45*
6	60	740	0.11
	100		0.19
	180		0.35*

*Test Reynolds number (Additional tests were made at other Re/in. values for models without control surfaces.)

For all coefficients the model planform area and diameter were used for the reference area and length, respectively. Moment coefficients were taken about the body mid-chord point (see Fig. 2), and the angles of attack were corrected for deflections of the sting support caused by air loads on the model. Axial force was corrected for the base axial force on the balance cavity.

PRECISION OF DATA

From the tunnel airflow calibration data and the known precision of pressure measuring instrumentation, the estimated uncertainties in the flow parameters are as follows:

<u>M</u>	<u>Calib. * M</u>	<u>p₀, psia</u>	<u>q, psia</u>
2	2.00 ± 0.01	±0.03	±0.02
3	3.00 ± 0.01	±0.06	±0.04
4	4.03 ± 0.01	±0.15	±0.05
5	5.09 ± 0.02	±0.30	±0.08
6	6.01 ± 0.02	±0.30	±0.04

* Mach number used in data reduction

Estimated uncertainties in the coefficients were determined from the balance calibration data and free-stream dynamic pressure q and are given here for Mach numbers 5 and 6. The values at Mach 5 are typical for the lower Mach numbers also.

M	C_L	C_D	C_m	C_Y	C_n	C_l
5	$\pm 3. \times 10^{-3}$	$\pm 0.7 \times 10^{-3}$	$\pm 0.24 \times 10^{-3}$	$\pm 2.6 \times 10^{-3}$	$\pm 0.38 \times 10^{-3}$	$\pm 0.07 \times 10^{-3}$
6	$\pm 5. \times 10^{-3}$	$\pm 1.1 \times 10^{-3}$	$\pm 0.39 \times 10^{-3}$	$\pm 4.2 \times 10^{-3}$	$\pm 0.46 \times 10^{-3}$	$\pm 0.11 \times 10^{-3}$

The sector positioning of the angle of attack was accurate to within ± 0.1 deg.

RESULTS

The longitudinal characteristics of the basic models at Mach 5, compared in Fig. 5, show that models B₂ and B₃, which had their point of maximum thickness at the trailing edge, were less unstable and had lower minimum drag than the symmetrical body shape B₁. The increase in drag and decrease in instability which resulted from blunting the edge radius of the symmetrical body (Model B₄) is also apparent. These trends were similar at the other Mach numbers, as is shown in Fig. 6, which presents the variation of several basic aerodynamic parameters with Mach number. The variation with Reynolds number of these parameters was negligible.

A significant amount of pitch control was obtained by the pitch-evators as shown in the data presented for models B₁ and B₃ at Mach 5 (Fig. 7). A comparison of models B₁ and B₃ with pitch-evators is given in Fig. 7a. These data illustrate the greater potential for trim of model B₃, and the figure shows that model B₃ with a 15-deg deflection on the aft pitch-evator trims out at the same lift coefficient as Model B₁ with 20-deg deflections on both pitch-evators. The decrease in effectiveness of the forward pitch-evator at angle of attack caused by the shielding effect of the body can be seen in the data presented in Fig. 7b. This figure shows the variation of pitch-evator effectiveness with deflection angle and includes data for forward and aft pitch-evators alone. The effectiveness of pitch-evators P₁, P₂, and P₃ are compared in Fig. 7c, and these data show that extending the pitch-evator chord (P₃) was more effective than extending the span (P₂). Also shown in Fig. 7 is the stabilizing effect of the lateral control surfaces (wedgevators and conevators) on the basic model B₃ (Fig. 7d).

Similar trends were obtained at the other test Mach numbers, as is shown in Fig. 8a for the relative effectiveness of pitch-evators P_1 , P_2 , and P_3 . The drag increase caused by the pitch-evators is also given in this figure (Fig. 8b), showing that the more effective pitch-evator P_3 (extended chord) gave about the same minimum drag as pitch-evator P_2 (extended span).

Lateral controls were tested on basic model B_3 only, and a plot of typical data at Mach 5 is presented in Fig. 9. These data (Fig. 9a) show the amount of directional control obtained by the wedgevators and the lateral stability characteristics of the model with conevators. Effective roll control was provided by both these devices (Fig. 9b).

Typical schlieren photographs (Fig. 10) show the flow patterns over the models with fore and aft pitch-evator deflections. The forward pitch-evators are masked by the test-section window frame, but the wake pattern over the top surface of the model is clearly evident as are the flow separations ahead of the aft pitch-evators. Several pictures of the model with lateral controls are also shown.

CONCLUSIONS

Results of the force tests of these lenticular configurations at supersonic speeds show that:

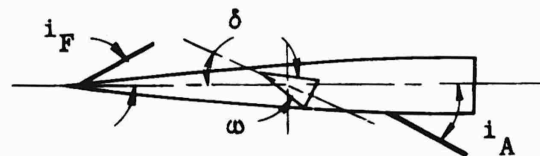
1. Optimum performance was obtained on Model B_3 ; however, all the models were longitudinally unstable.
2. The methods used for longitudinal and lateral control were effective.

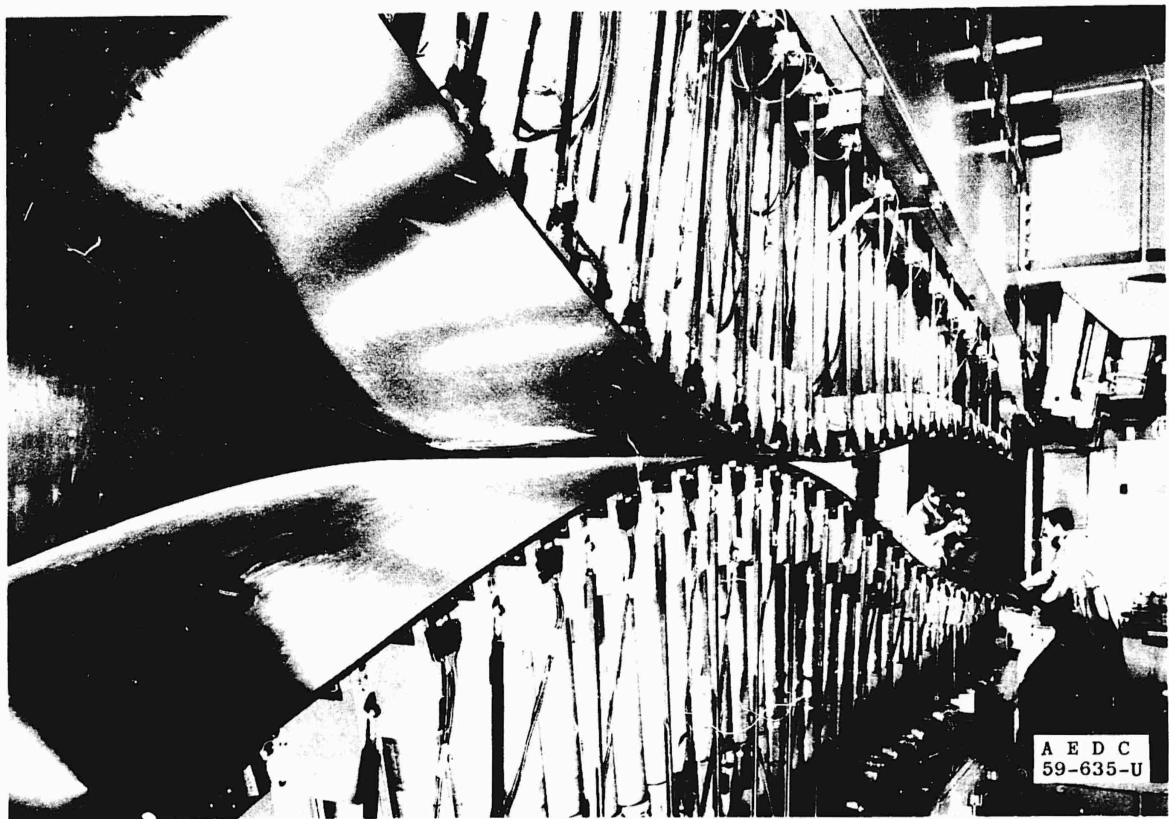
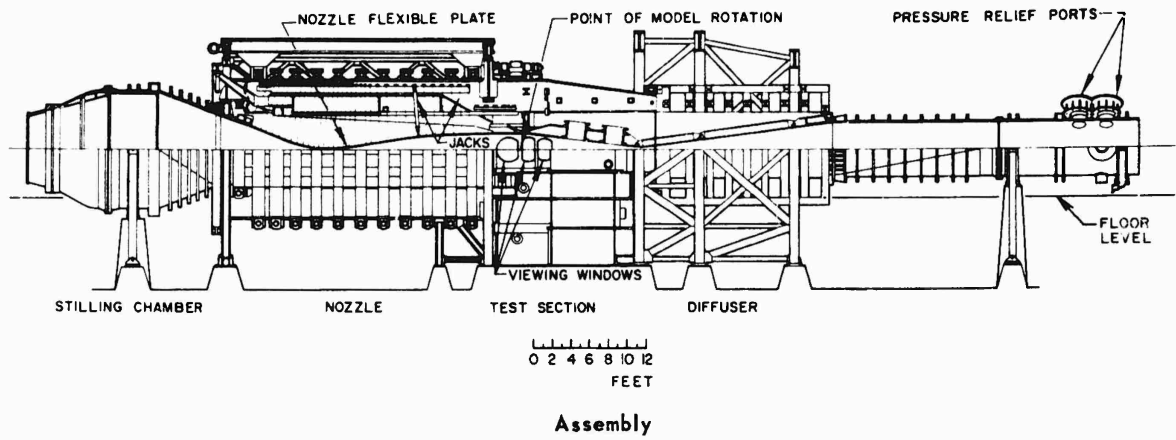
REFERENCES

1. Anderson, A. "Aerodynamic Test Results of Two Configurations of a Proposed Bomber Defense Missile at Supersonic Speeds." AEDC-TN-58-72, October 1958. (Secret)
2. Anderson, A. "Stability Tests of Three Lenticular Models at Supersonic Speeds." AEDC-TN-59-99, September 1959. (Secret)
3. Anderson, A. "Stability and Control Characteristics of Seven Lenticular Models at Mach Number 5." AEDC-TN-59-162, January 1960. (Secret)
4. Schueler, C. J. and Strike, W. T. "Calibration of a 40-Inch Continuous Flow Tunnel at Mach Numbers 1.5 to 6." AEDC-TN-59-136, November 1959.

TABLE 1
SUMMARY OF TEST CONFIGURATIONS

Model	i_F/i_A	ω_L/ω_R	δ_L/δ_R	ϕ			M					
				0	180	90	2	3	4	5	6	
B ₁ P ₁	0/0	-	-	x	x	x	x	x	x	x	x	x
	9/20			x	x				x	x		
	20/0			x	x						x	x
	20/20			x	x				x	x	x	x
B ₂ P ₁	0/0			x	x	x	x	x	x	x		
	20/20			x	x		x	x			x	
B ₃ P ₁	0/0			x	x	x	x	x	x	x	x	
	0/20			x	x		x	x	x	x	x	
	20/0			x	x				x	x		
	20/20			x	x		x	x	x	x	x	
	0/15			x	x		x	x	x	x		
	15/15			x	x		x	x	x	x		
	0/25			x	x		x	x	x	x		
B ₃ P ₂	25/25			x	x		x	x	x	x		
	0/20			x	x		x	x	x	x		
B ₃ P ₃	20/20			x	x		x	x	x	x		
	0/20			x	x		x	x	x	x		
B ₁ P ₁ B ₃ P ₁ W	20/20			x	x		x	x	x	x		
	0/0	15/15	0/0	x		x	x	x	x	x		
	0/0		10/10	x		x	x		x	x		
			15/15	x		x		x	x	x		
			20/20	x		x	x		x	x		
		30/15	0/0	x		x			x	x		
			10/10	x		x	x					
			15/15	x		x			x	x		
		45/15	0/0	x		x	x	x	x	x		
			10/10	x		x	x					
			15/15	x		x	x	x	x	x		
		0/20	15/15	0/0	x	x		x	x	x	x	
		0/25	45/15	10/10	x			x	x	x	x	
	B ₃ P ₃ W B ₃ P ₁ C	0/20	15/15	0/0	x	x		x	x		x	x
		0/0	30/30	0/0	x		x	x	x	x	x	
			0/20	x		x	x	x				
			10/10	x		x	x	x	x	x		
0/20		30/30	0/0	x	x		x	x	x	x		





Nozzle and Test Section

Fig. 1. Tunnel A, a 40 by 40-in. Supersonic Wind Tunnel

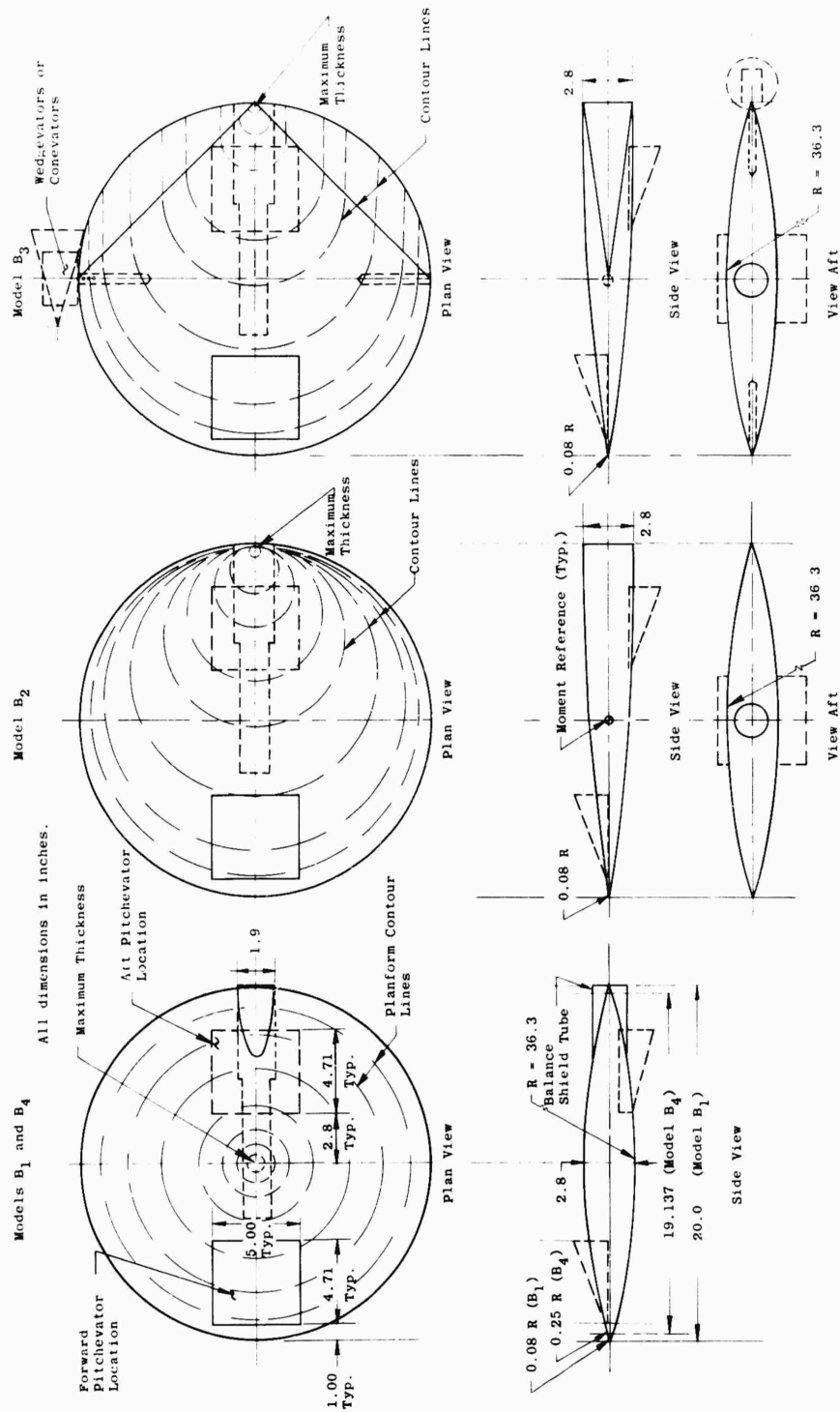
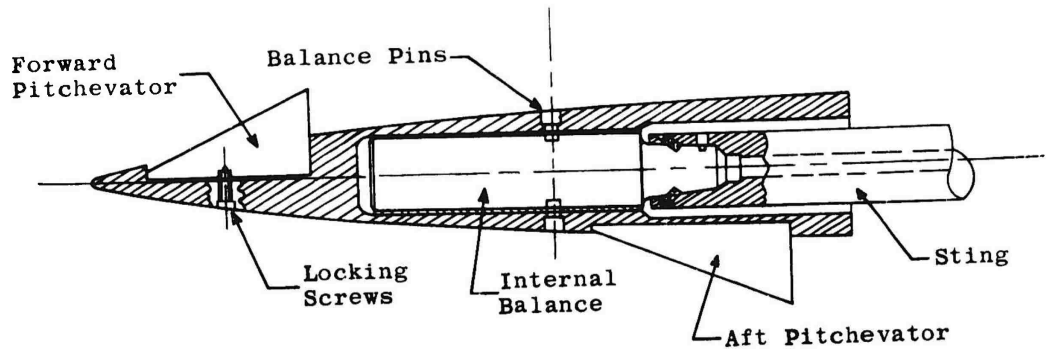
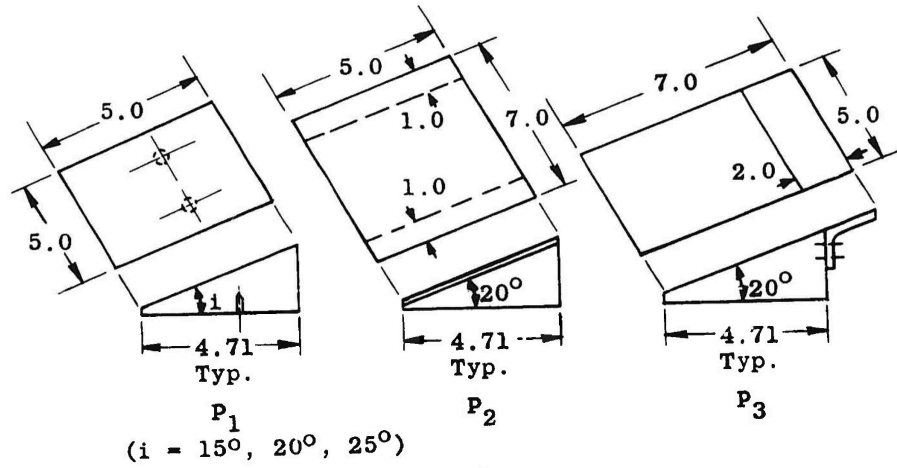


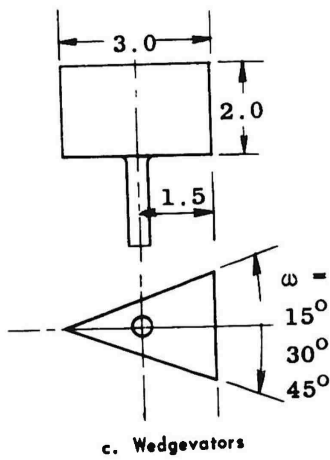
Fig. 2 Sketches of Models



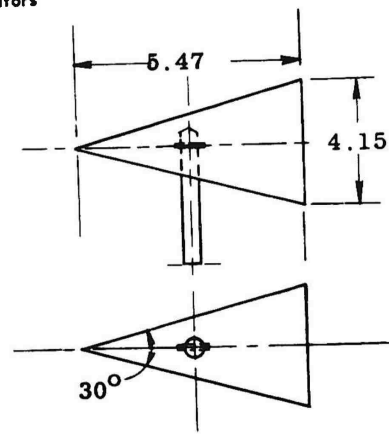
a. Typical Model Installation



b. Pitchevators

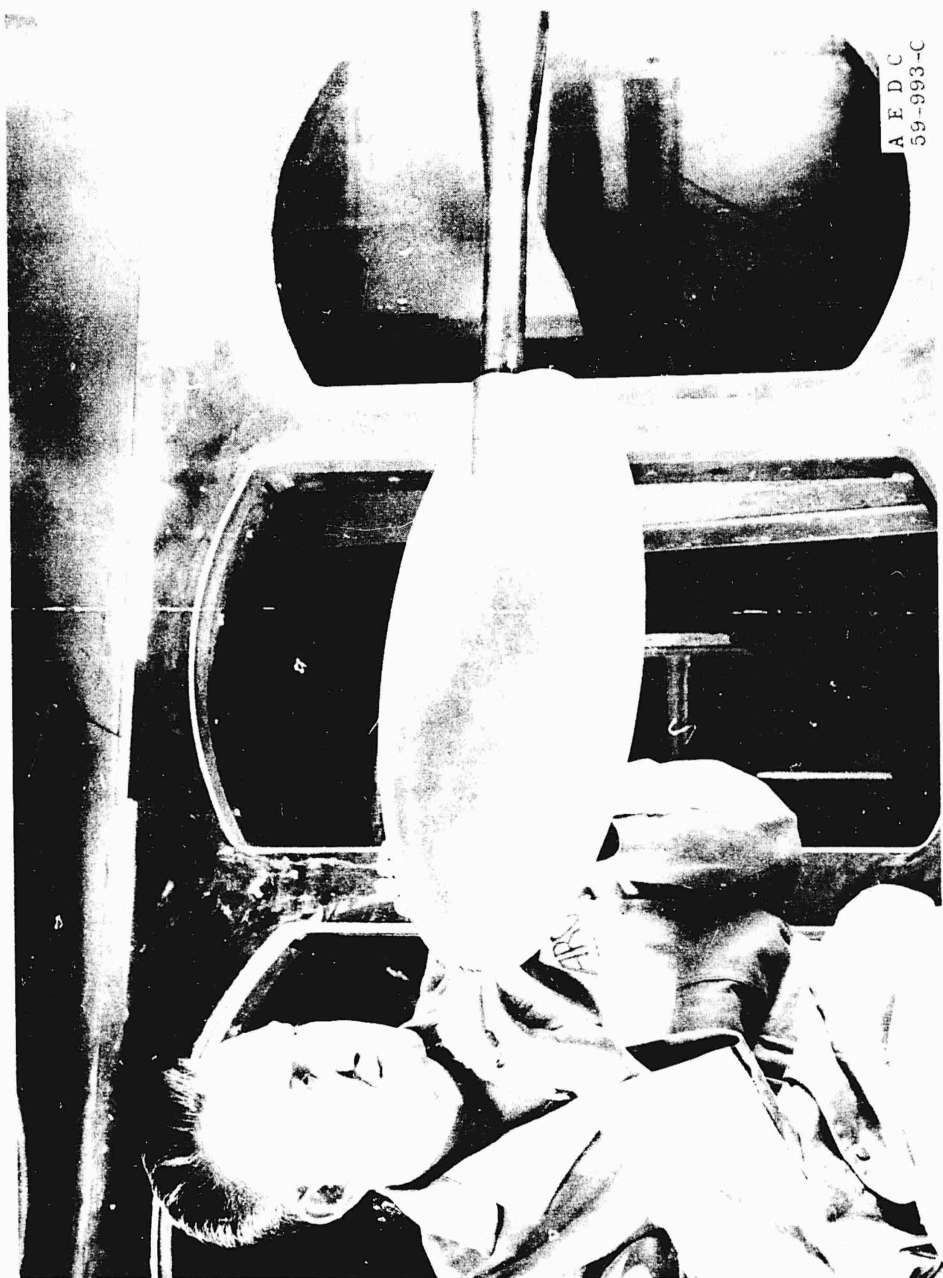


c. Wedgevators



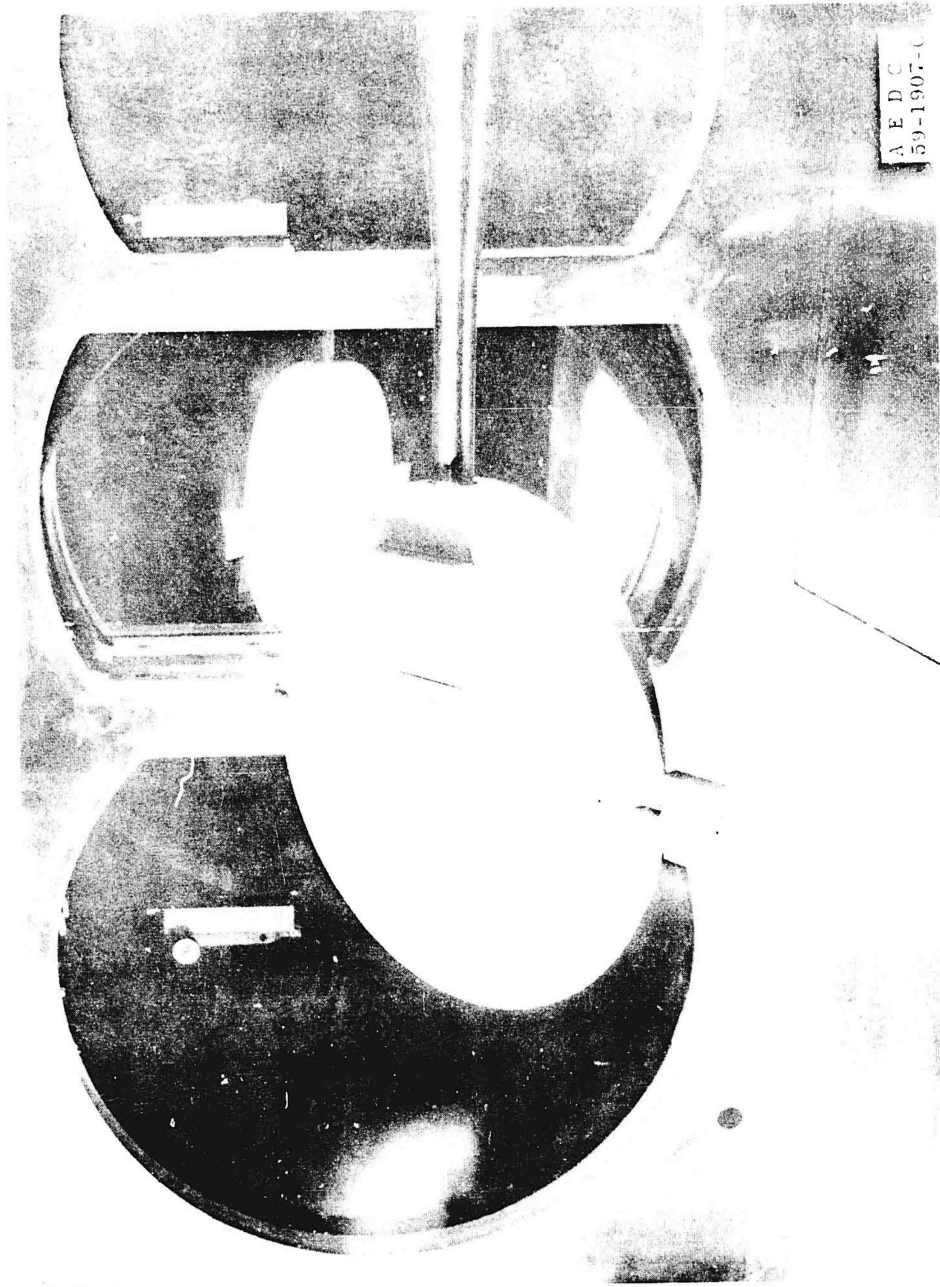
d. Conevators

Fig. 3 Sketches of Typical Model Installation and Model Components



a. Model B₁, Configuration B₁P₁0/0

Fig. 4 Model Photographs



b. Model B₃, Configuration B₃P₁W₀/20, 15/15, 0/0

Fig. 4 Concluded

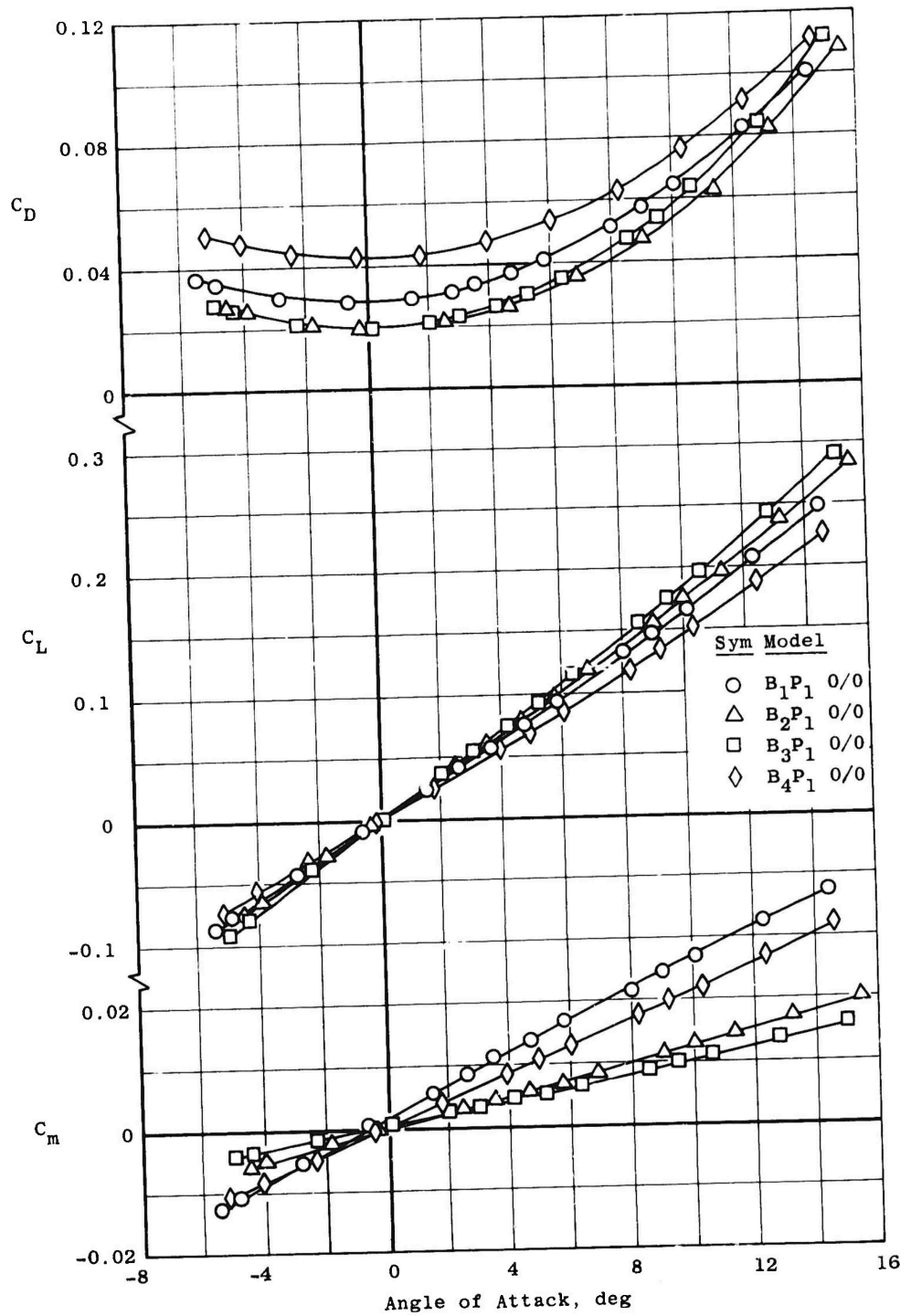


Fig. 5 Longitudinal Characteristics of Basic Models at Mach 5

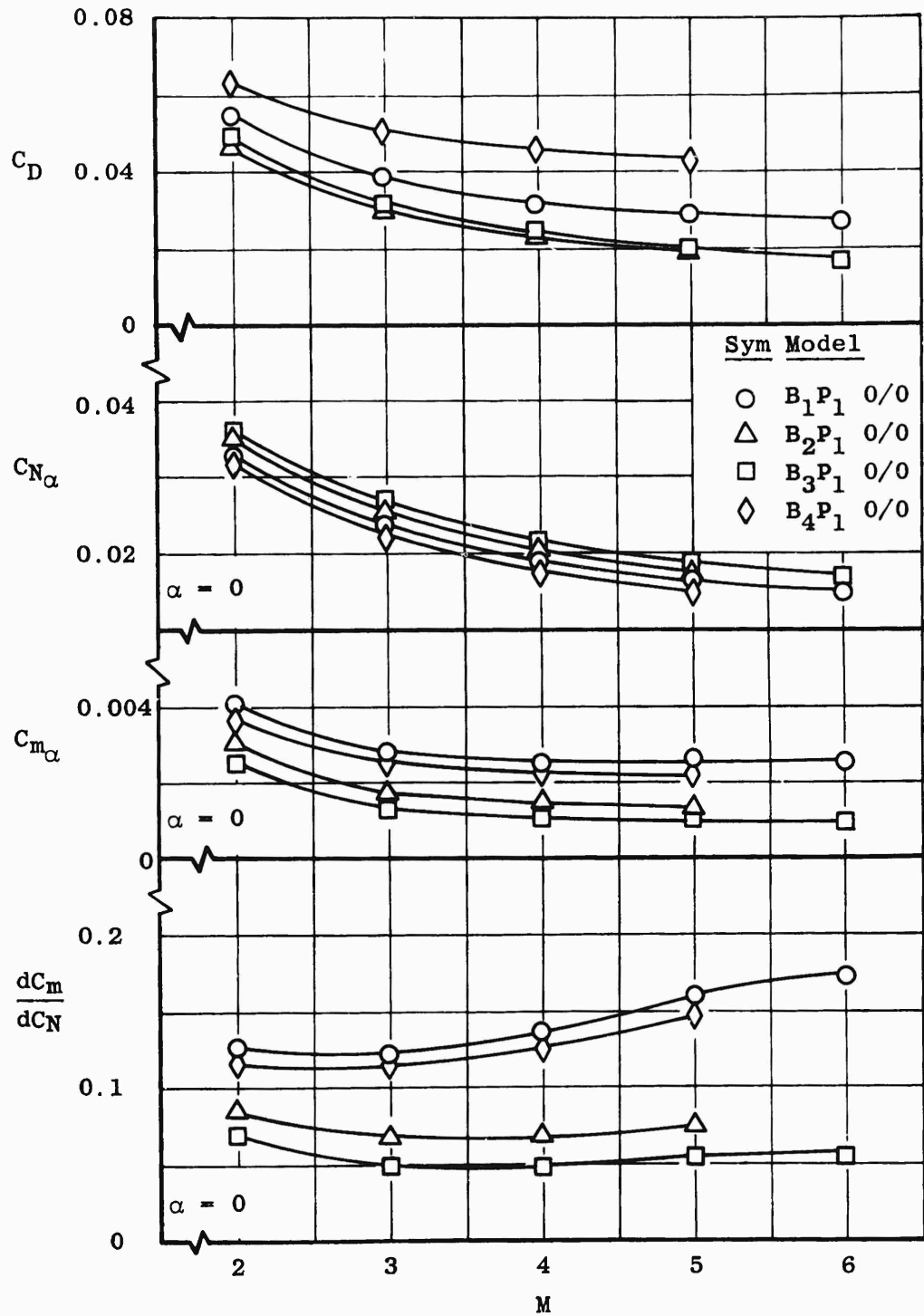


Fig. 6 Variation of Model Aerodynamic Parameters with Mach Number

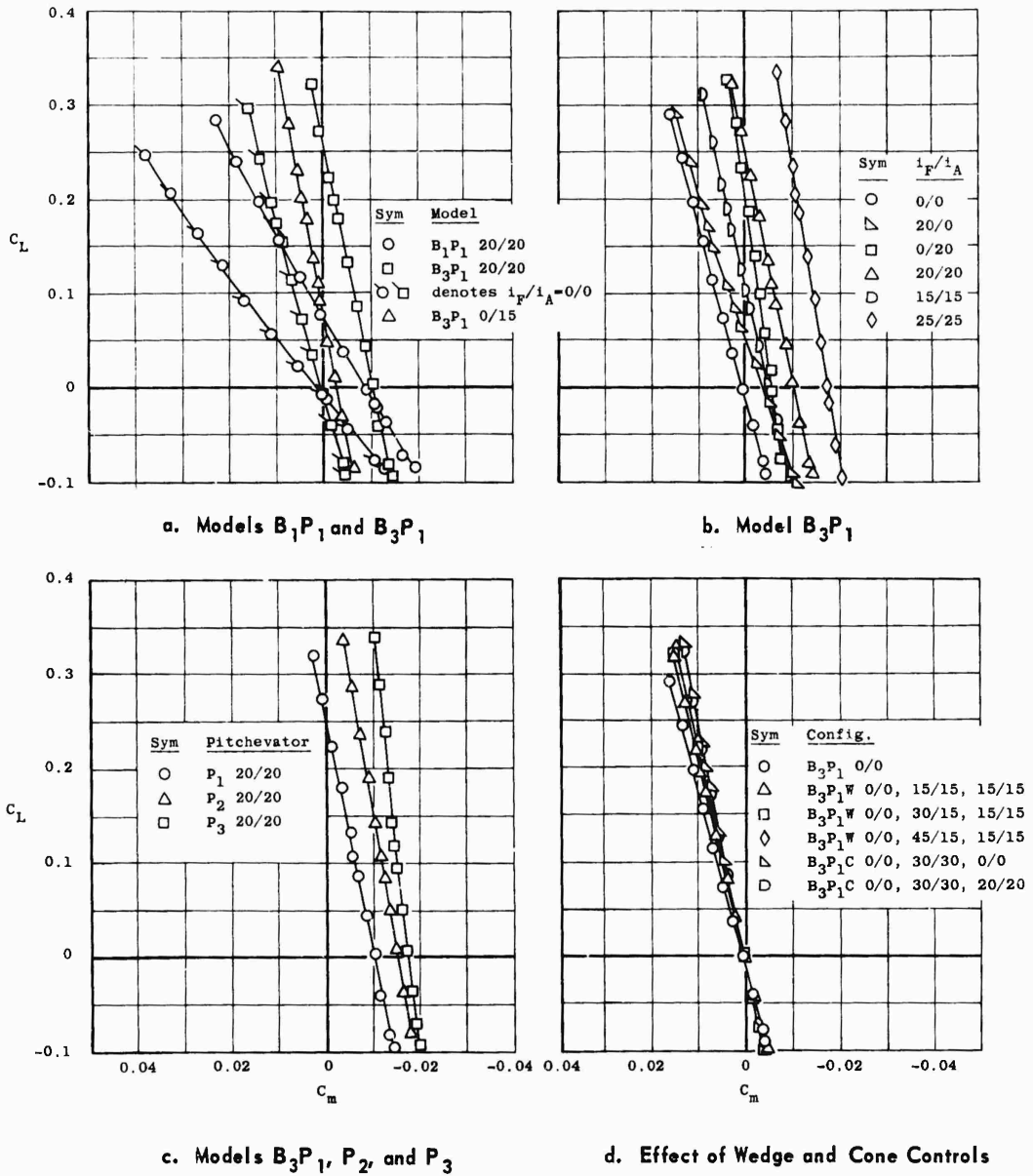
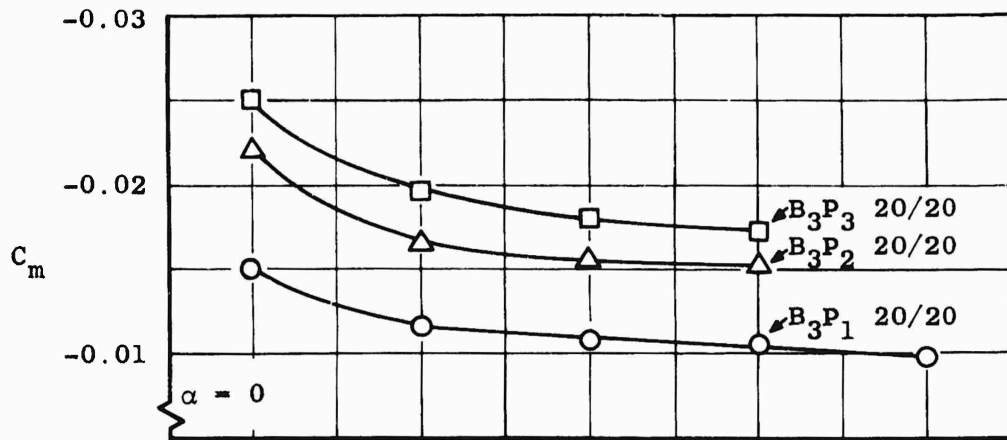
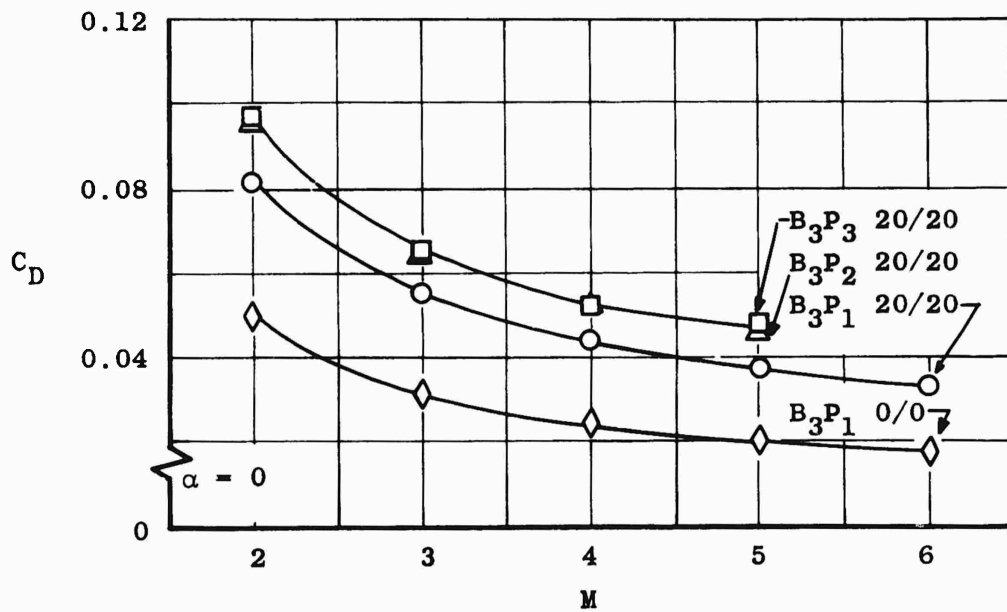


Fig. 7 Longitudinal Stability and Control Characteristics at Mach 5

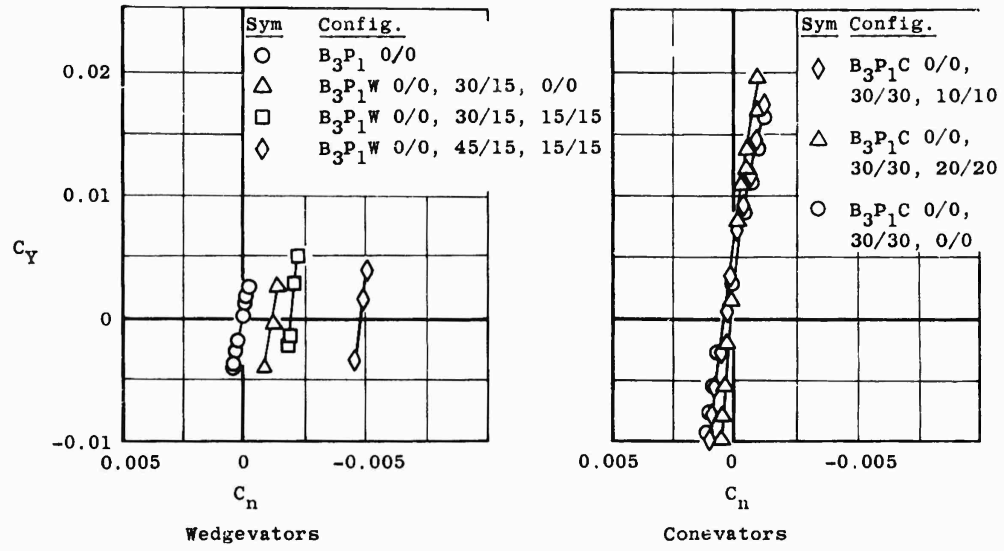


a. Moment Coefficient at $\alpha = 0$

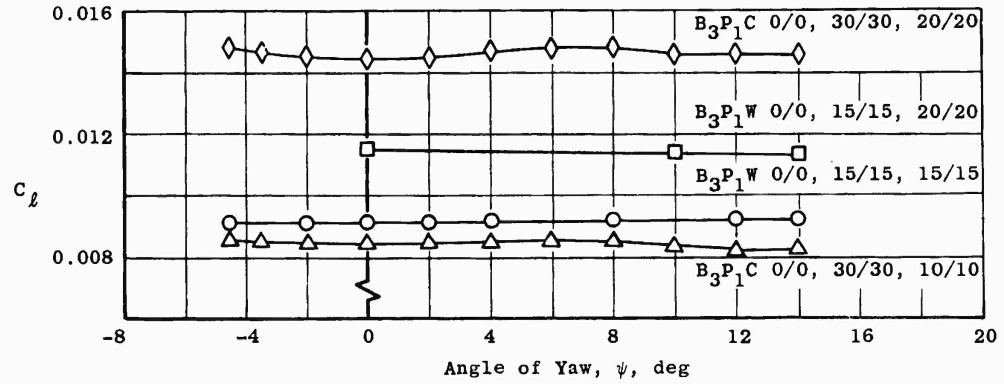


b. Minimum Drag Coefficient

Fig. 8 Variation of Pitchvator Effectiveness with Mach Number



a. Directional Stability and Control



b. Roll Control

Fig. 9 Lateral Stability and Control Characteristics at Mach 5, Model B₃

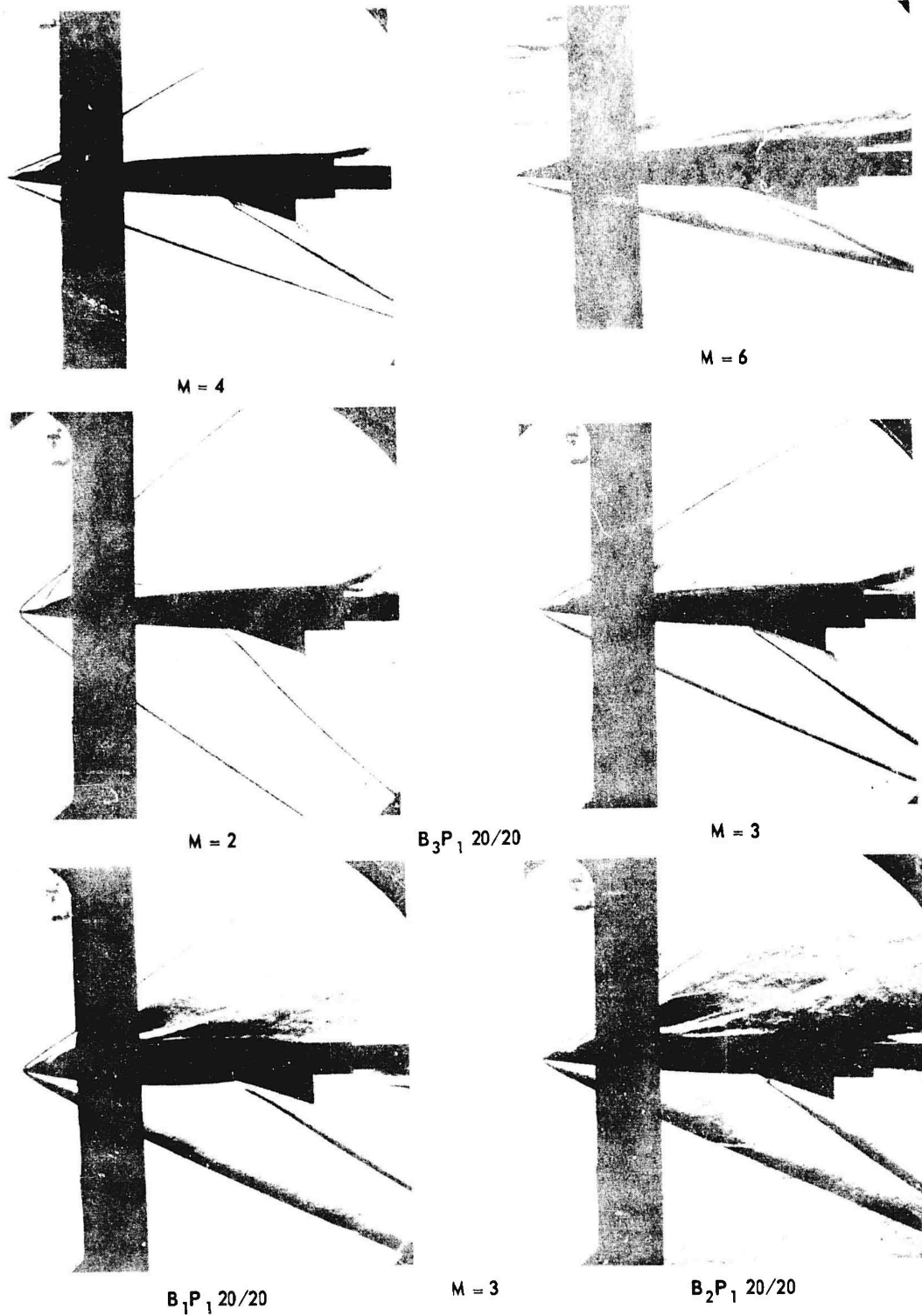
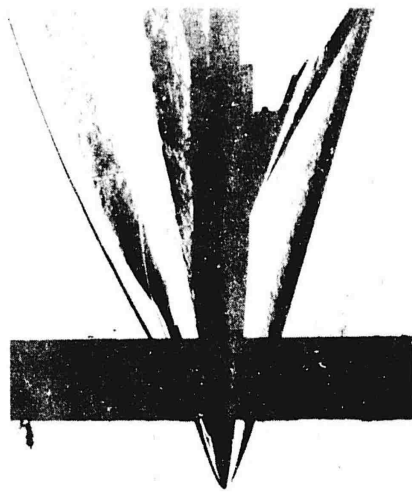
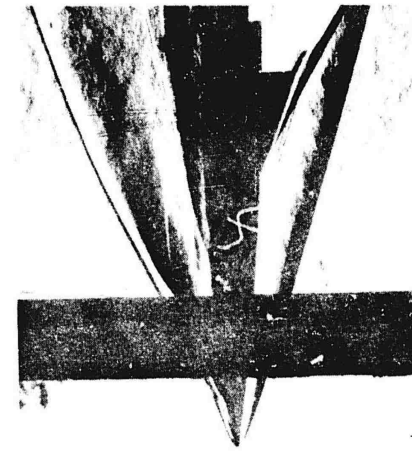


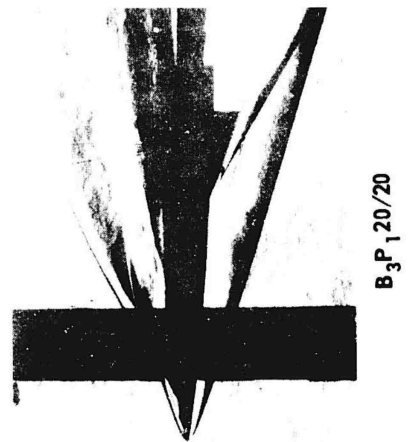
Fig. 10 Typical Schlieren Photographs



$B_3P_3 20/20$



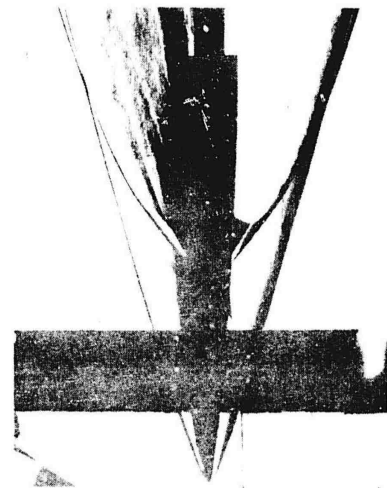
$B_3P_2 20/20$



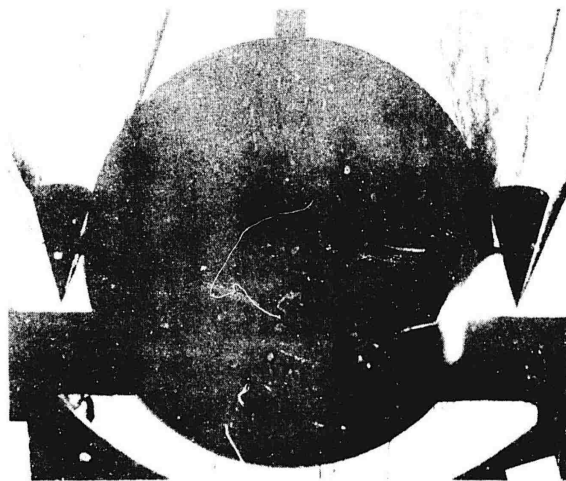
$B_3P_1 20/20$



$B_3P_1W 0/0, 30/15, 15/15 (\phi = 30^\circ)$



$B_3P_1C 0/0, 30/30, 20/20 (\phi = -90^\circ)$



$B_3P_1C 0/0, 30/30, 20/20 (\phi = 0^\circ)$

Fig. 10 Concluded